Design of Frequency Reconfigurable Antenna on Dielectric and Magnetic Metamaterial Composite Substrate

Mousa Al-Omari, Hussein Attia, Khurram K. Qureshi, and Sharif I. M. Sheikh

***Abstract*—Reconfigurable planar antennas are essential in multifunctional wireless communication devices. This paper presents the design of a frequency reconfigurable patch antenna printed on a composite substrate made of a dielectric and a magnetic metamaterial (MMM). The MMM comprises magnetized ferrite slabs with embedded split-ring resonators (SRR). The constructive coupling between the resonances of the magnetized ferrites and SRR is optimized to achieve promising reconfigurable properties. The proposed frequency reconfigurable antenna demonstrates a 158% increase in the frequency tuning range. Furthermore, the simulated results are experimentally verified, and the composite substrate shows slight effects on the antenna radiation characteristics.**

***Index Terms*—Reconfigurable Antenna, Ferrite, Metamaterials, Planar Antenna.**

I. Introduction

Reconfigurable antennas play an important role in maximizing the performance of multifunctional wireless communication devices [1] - [2]. Frequency reconfigurable antennas facilitate frequency hopping and dynamic spectrum allocation, while pattern reconfiguration can increase channel capacity by reducing in-band interference [3]. Popular techniques to reconfigure antenna resonant frequency [4]–[9] or radiation pattern [10], [11] employ integrated PIN/varactor diodes or MEMs switches to alter the effective length or current distribution of the radiating element.

Recent multifunctional printed antennas use optimally positioned PIN diodes to reconfigure both frequency and radiation patterns [12]–[15]. However, most of these antennas are limited by unwanted interference and a complicated switching mechanism. Although relatively simple switching circuits are used in designing wide-band pattern reconfigurable antenna, the out-of-band interference often limits the transceiver performance [16], [17]. Anisotropic substrates and superstrates are also popular in the design of reconfigurable microstrip antennas [18], [19]. Popular substrates include ferrites [20], [21] or liquid crystals [22], [23], where externally applied static magnetic or electric fields change the effective permeability or permittivity of the antenna, respectively. Magnetized ferrites are popular in microwave circuits and devices. The mechanism requires an externally applied static magnetic field (H_{DC}) to control the gyrotropic interaction between the propagating EM wave and the ferrite material [24]. Ferrite-based reconfigurable antennas are mostly limited by the size of the magnets needed to excite H_{DC} [25], [26]. A recent solution to this problem is integrating the magnetizing coils within the ferrite substrate using low-temperature co-fired ceramics (LTCC) technique [27]. Another method of reducing the required H_{DC} is enhancing the gyromagnetic interaction by incorporating metamaterial cells within the ferrite medium [28]–[30].

In this paper, H_{DC} requirement is reduced by optimally integrating split-ring resonators (SRR) within the magnetized ferrite material to allow constructive coupling between the SRR and ferrimagnetic resonances. SRR is a popular metamaterial unit cell, made of two enclosed metallic C-rings with gaps positioned on opposite sides [31]. When an SRR is energized by an external magnetic field, the induced currents on the C-rings change the resonant properties of the structure [32]. Thus, SRR shapes, dimensions, and integration methods play an essential role in constructively affecting the magnetic properties of SRR-integrated ferrite material, called here as magnetic-metamaterial (MMM). A patch antenna based on a dielectric-MMM composite substrate is designed to demonstrate the reduced magnetization requirements (H_{DC}) to achieve a wider range of frequency reconfiguration. The commercial simulator (HFSS) is used to design and optimize the proposed reconfigurable antenna, and a prototype of the antenna is fabricated and tested to verify the simulated results.

II. Design of ferrite-embedded antenna

A microstrip antenna operating around 4 GHz, shown in Fig. 1, is designed on a dielectric-ferrite composite substrate. To achieve reconfigurability with minimum insertion-loss, the dimensions of the embedded ferrite slabs are kept to a minimum. The dielectric part of the substrate is chosen as Rogers RT/duroid 5880 material with a relative permittivity of 2.2, thickness of 3.2 mm, and loss tangent of 0.0009. The ferrite part of the substrate is NG-1850 microwave ferrite [33] with saturation magnetization of 1850 Gauss, a dielectric constant of 14.8, and thickness of 3.2 mm.

The ferrite slabs are positioned under the central part of the patch and close to the non-radiating edges to allow adequate gyromagnetic interaction between the ferrite and the H-field generated inside the substrate. For an unmagnetized ferrite

This work was supported by the Deanship of Research Oversight and Coordination (DROC) at KFUPM under the Interdisciplinary Research Center for Communication Systems and Sensing through Project INCS2106.

Mousa Al-Omari, Hussein Attia, Khurram K. Qureshi and Sharif Sheikh are with the Center for Communication Systems and Sensing, and the Electrical Engineering Department at King Fahd University of Petroleum & Minerals (KFUPM), Dhahran, 31261, Saudi Arabia.

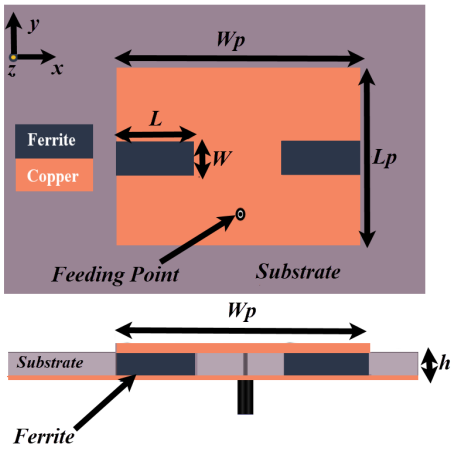

Fig. 1: The proposed frequency reconfigurable patch antenna printed on a dielectric-ferrite composite substrate (Lp = 22.5 mm, Wp = 26 mm).

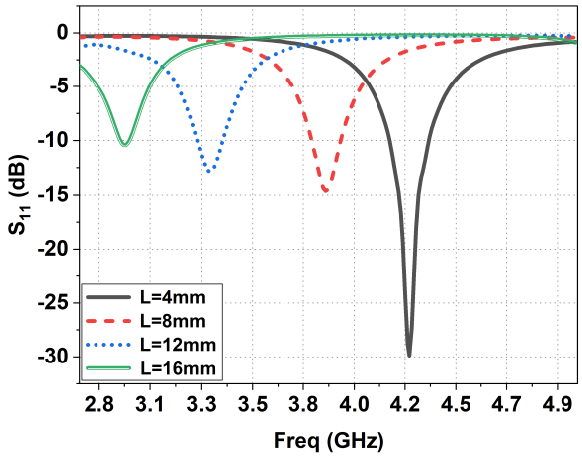

Fig. 2: Reflection coefficient of the ferrite-embedded antenna with changing the length (L) of the unmagnetized ferrite slab embedded in the substrate.

slab, the selection of its length (L) and width (W) is dependent on the desired resonance frequency and gain of the antenna. The simulated reflection coefficients (S_{11}) of the antenna for different values of length (L) and the same width (W = 4 mm) are plotted in Fig. 2. Note that increasing the length of the ferrite slab by about 12 mm (i.e., from 4 to 16 mm) can reduce the resonant frequency by 30%, often at the cost of increased insertion-loss. Similar changes of ferrite width (W) exhibit a negligible effect on the resonant behavior due to less gyromagnetic interaction between the ferrite material and the magnetic field component of the EM wave.

To implement frequency reconfigurability in the designed antenna, an external static magnetic field (H_{DC}) is applied orthogonally on the ferrite slabs. The gyromagnetic property of ferrite is expressed by the tensor permeability [μ_r] [34], [35]

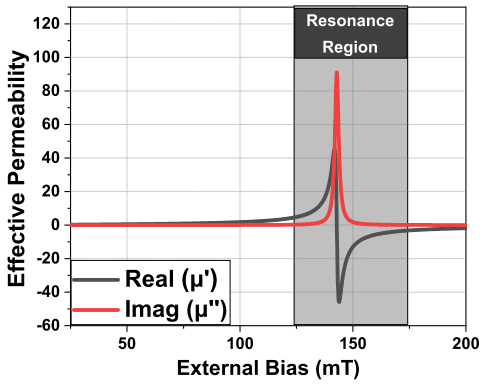

Fig. 3: Resonance regions of a magnetized NG-1850 ferrite (γ =2.8, 4πMs=1850G, ϵ_r = 14.8).

$$[\mu_r]=\begin{bmatrix} 1+\frac{\gamma^2.(H_{DC}-MN_z).(MN_z)}{\gamma^2(H_{DC}-MN_z)^2-f^2} & \frac{-\gamma.(MN_z).f}{\gamma^2(H_{DC}-MN_z)^2-f^2} & 1 \\ \frac{\gamma.(MN_z).f}{\gamma^2(H_{DC}-MN_z)^2-f^2} & 1+\frac{\gamma^2.(H_{DC}-MN_z).(MN_z)}{\gamma^2(H_{DC}-MN_z)^2-f^2} & 1 \\ 1 & 1 & \mu_z \end{bmatrix} \quad (1)$$

Where f is the frequency of the propagating signal and γ, M and N_z are the gyromagnetic-ratio, magnetization, and demagnetization-factors of the ferrite material, respectively.

The related effective permeability (μ_{eff}) of a magnetized ferrite material can be expressed as [35]

$$\mu_{eff}=\left(1+\frac{\gamma^2\cdot(H_{ex}-MN_z)\cdot(MN_z)}{\gamma^2(H_{ex}-MN_z)^2-f^2}\right)\left[1-\left(\frac{\gamma\cdot(MN_z)\cdot f}{\gamma^2\cdot(H_{ex}-MN_z)\cdot(MN_z)}\right)^2\right] \quad (2)$$

Figure 3 shows the change in the effective permeability (μ_{eff}) of the NG-1850 ferrite material with changing the magnetizing field (H_{DC}) at 4 GHz. Note that the regions close to lossy ferrimagnetic resonance demonstrate a large change in μ_{eff} for a slight change in H_{DC}. Thus, selecting the ferrite operating region is critical to establish a balance between insertion-loss and magnetic biasing requirements. Hence, and to avoid further losses, the operating region of the proposed ferrite-embedded antenna will be outside the resonance region when $H_{DC} \leq$ 125 mT as seen in Fig. 3.

For externally magnetized ferrite slabs with dimensions of L= 8 mm and W= 4 mm, the change in resonant frequencies with changing magnetization fields (H_{DC}) is plotted in Fig. 4. This figure was produced using HFSS by applying a uniform magnetic bias excitation H_{DC} to both ferrite pieces. The permeability tensor rotation angles were assigned in HFSS to control the direction of the applied H_{DC}. The designed antenna demonstrates a frequency tuning of Δf_r = 260 MHz for ΔH_{DC} = 50.2 mT, where the antenna gain changed from 7.7 dB at H_{DC} = 0 to 7.1 dB at H_{DC} = 50.2 mT. Note that the ferrite slabs are magnetized in opposite directions to maximize the gyromagnetic interaction and related frequency reconfigurable properties of the antenna. Simulated results have also shown that doubling ΔH_{DC} increases Δf_r by 3.5 times at the cost of a larger magnetizing network.

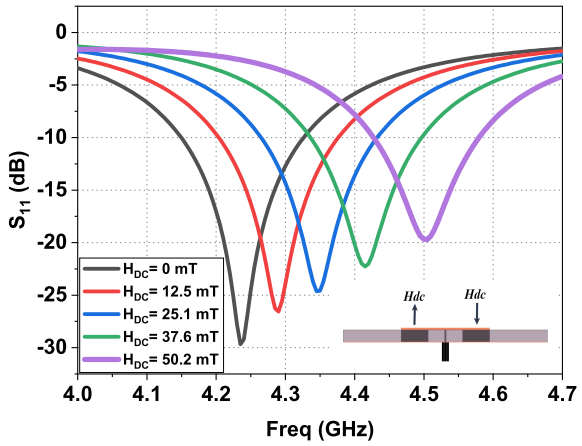

Fig. 4: Resonance frequency tuning of the ferrite-embedded antenna corresponding to the magnetizing field (H_{DC}).

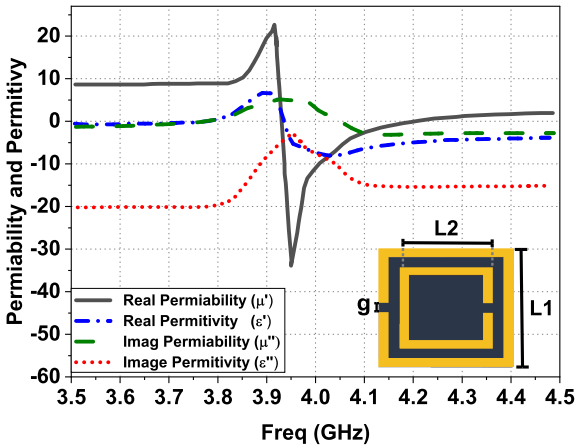

Fig. 5: Simulated real and imaginary parts of the effective permeability and permittivity of SRR structure.

III. Design of Magnetic Metamaterial Antenna

To achieve greater reconfigurable capabilities with smaller H_{DC}, MMM is proposed in this work. The designed MMM integrates SRRs within the magnetized ferrite slab to improve the gyromagnetic properties. However, optimal integration of SRR within the magnetized ferrite material requires a thorough understanding of their magnetic properties. SRRs are widely used in metamaterial substrates to influence the constitutive parameters of the antenna. The resonant frequency of this structure depends on the substrate properties and the dimensions of the concentric C-shaped square metal loops with gaps located at the opposite ends. When exposed to an external magnetic field, induced currents in the metal loops cause resonance similar to that of magnetic dipoles within magnetized ferrites.

Herein, MMM is realized by optimally integrating SRR within a magnetized ferrite substrate to introduce constructive coupling between the SRR and ferrite resonances. The aim is to achieve wider tunable material properties with the same magnetic biasing (H_{DC}) requirements. In this work, conductive SRRs are designed and optimally implanted within the ferrite material to operate around 4 GHz. The dimensions of the ferrite-based SRR, seen in Fig. 5, have been numerically optimized and found to be *L1* = 3.2 mm, *L2* = 2.7 mm, g = 0.3 mm to achieve resonance around 4 GHz. The simulated real and imaginary effective permeability and permittivity of the SRR structure are plotted in Fig. 5 where a higher effective permeability is observed around 3.9 GHz, which is very close to the antenna resonant frequency.

Oppositely oriented SRRs are integrated into the magnetized ferrite slabs to maximize magnetic interaction with the EM waves. Figure 6 shows the reconfigurable patch antenna based on a composite dielectric and MMM substrate. Also, Fig. 6 depicts the changes in antenna resonance for different locations of the SRRs inserted at a distance d from the inner edge of unmagnetized ferrite slabs. In this design, d = 7 mm is selected to achieve improved antenna performance throughout the whole operating range. Figure 7 depicts the frequency reconfigurability of the SRR-MMM-integrated antenna for

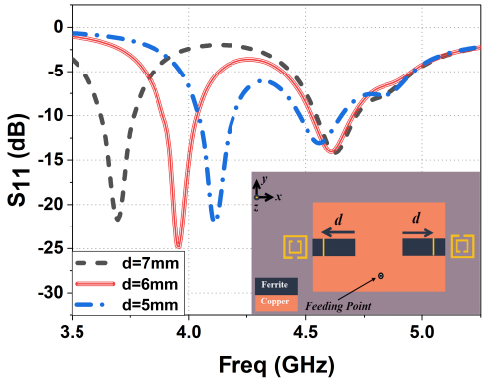

Fig. 6: Reflection coefficients of the MMM-based patch antenna for different positions (d) of the SRRs within the ferrite slabs.

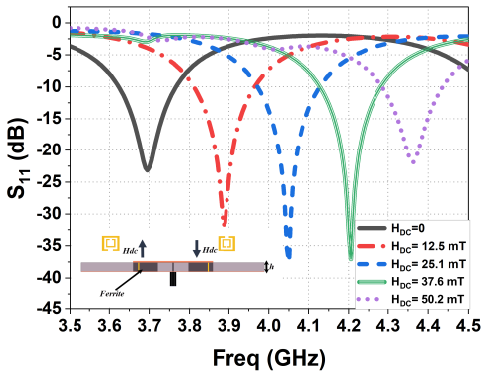

Fig. 7: Improved frequency reconfigurability of the MMM-based patch antenna with d=7 mm and five values of H_{DC}.

different values of the external magnetizing field (H_{DC}). The achieved frequency tuning range is 3.69-4.36 GHz (i.e., Δf_r=670 MHz). Note that the SRR-based antenna demonstrates a 158% improvement in frequency tuning compared with Δf_r=260 MHz (see Fig. 4) in the absence of SRR for the same magnetization range of ΔH_{DC} = 50.2 mT .

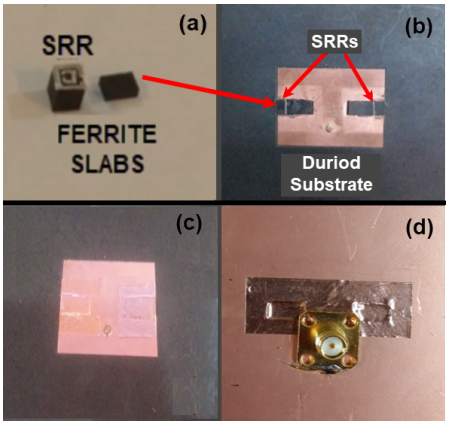

Fig. 8: Fabricated antenna (a) Ferrite slabs with SRR, (b) Proposed antenna with integrated ferrite-SRR, (c) Top view of the antenna with copper tape covering the ferrite slabs, (d) Bottom view of the antenna with copper tape.

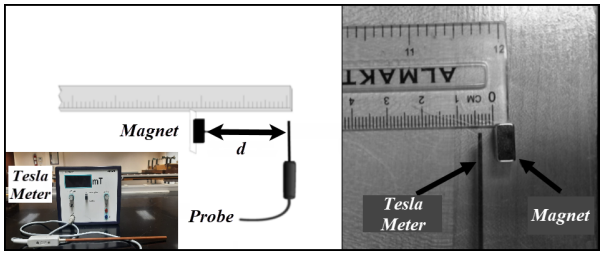

Fig. 9: Magnetic field measurement of the NdFeB magnet using Tesla-meter.

IV. Fabrication and Measurements

To validate the enhanced performance of the reconfigurable antenna, the antenna was fabricated using a 3.2-mm-thick RT/Duroid substrate (ϵ_r=2.2) as seen in Fig. 8. Two rectangular cavities (i.e., holes) of size 8x4x3.2 mm^3 are engraved in the substrate, and two SRR-embedded ferrite slabs with the same dimensions have been inserted into these cavities. The ferrite slabs have been covered on both sides with copper tapes, as seen in Fig. 8(c) and (d).

To provide the external magnetizing field experimentally, a coil can be used by controlling its current to generate the required magnetic field to bias the ferrite slabs. On the other hand, permanent magnets with some mechanical movement mechanism can be used to magnetize the ferrite. Hence, NdFeB magnets with (10×10×5) mm^3 dimensions (known as N-42 type magnet) [36] have been placed at some distance form the SRR-embedded ferrite slabs to provide the required magnetic field. To control the magnetic field intensity of the NdFeB magnets, the distance between the magnet and the antenna is changed. The generated magnetic field has been measured using a Tesla-meter as shown in Fig. 9.

The frequency reconfigurability capability of the fabricated antenna at H_{DC} = 0, 25.1 mT, and 50.2 mT is shown in Fig. 10. Good agreement between the simulated and measured results is clear. This figure shows that the experimental tuning range is 630 MHz compared to 670 MHz of the simulated one.

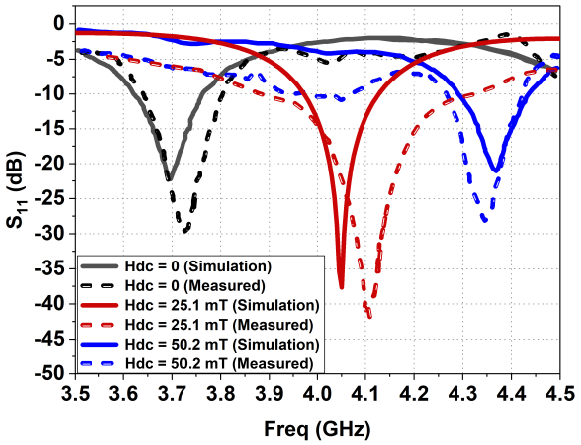

Fig. 10: Measured and simulated reflection coefficients of the proposed antenna when H_{DC} = 0, 25.1 mT, and 50.2 mT.

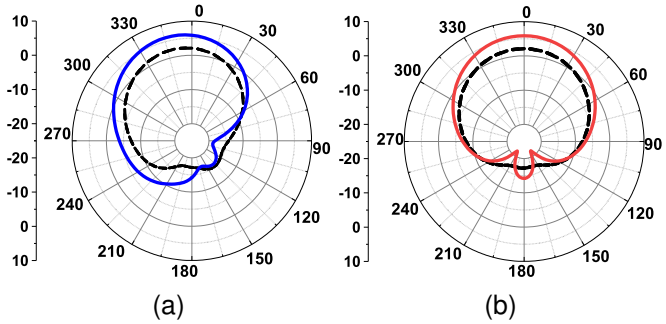

Fig. 11: Measured (dash) and simulated (solid) radiation patterns of the proposed antenna for H_{DC} = 50.2 mT at 4.37 GHz (a) E-Plane (left) and (b) H-plane (right).

Figure 11 shows the measured and simulated radiation patterns in the E- and H-planes at 4.37 GHz for H_{DC} = 50.2 mT. The observed slight discrepancy between the simulated and measured results is due to human error during the fabrication, structure assembly, and magnet biasing process, and ferrite losses differences between simulation and measurements. The antenna radiation efficiency ranges from 67-77% when the external magnetic bias changes from 0 to 50.2 mT.

V. Conclusions

The design of a novel magnetic metamaterial-based frequency reconfigurable microstrip antenna is presented. SRR structures are optimally integrated within the ferrite-embedded substrate to efficiently couple their resonances and reduce the required magnetic biasing for reconfiguration. Integrating a single SRR per ferrite slab improved the resonant tuning range by 158% for a magnetic biasing range of ΔH_{DC}=50.2 mT while maintaining an average efficiency of 72%. The experimental results corroborated the simulated frequency reconfigurable properties of the antenna.

References

[1] S. Gaya, R. Hussain, M. S. Sharawi, and H. Attia, "Pattern reconfigurable Yagi-Uda antenna with seven switchable beams for WiMAX

application," *Microwave and Optical Technology Letters*, vol. 62, no. 3, pp. 1329–1334, 2020.

[2] M. Ali, *Reconfigurable Antenna Design and Analysis*. Artech House, 2021.

[3] J.-I. Oh, J.-W. Kim, S. H. Han, S. Kim, J.-W. Yu, and I.-J. Hwang, "Pattern reconfigurable dual-polarized dipole antenna with staggered parasitic elements," *IEEE Access*, pp. 1–1, 2022.

[4] Y. Xu, Y. Tian, B. Zhang, J. Duan, and L. Yan, "A novel RF MEMS switch on frequency reconfigurable antenna application," *Microsystem Technologies*, vol. 24, p. 3833–3841, 2018.

[5] S. W. Lee and Y. Sung, "Compact frequency reconfigurable antenna for LTE/WWAN mobile handset applications," *IEEE Transactions on Antennas and Propagation*, vol. 63, no. 10, pp. 4572–4577, 2015.

[6] A. Khidre, F. Yang, and A. Z. Elsherbeni, "A patch antenna with a varactor-loaded slot for reconfigurable dual-band operation," *IEEE Transactions on Antennas and Propagation*, vol. 63, no. 2, pp. 755–760, 2015.

[7] A. Andy, P. Alizadeh, K. Z. Rajab, T. Kreouzis, and R. Donnan, "An optically-switched frequency reconfigurable antenna for cognitive radio applications," in *2016 10th European Conference on Antennas and Propagation (EuCAP)*, 2016, pp. 1–4.

[8] C. won Jung, M. jer Lee, G. Li, and F. De Flaviis, "Reconfigurable scan-beam single-arm spiral antenna integrated with RF-MEMS switches," *IEEE Transactions on Antennas and Propagation*, vol. 54, no. 2, pp. 455–463, 2006.

[9] M. A. Al-Omari and S. S. Iqbal, "Pattern reconfigurable magnetic-metamaterial-based microstrip antenna," in *2017 International Conference on Electrical and Computing Technologies and Applications (ICECTA)*, 2017, pp. 1–4.

[10] S.-L. Chen, P.-Y. Qin, W. Lin, and Y. J. Guo, "Pattern-reconfigurable antenna with five switchable beams in elevation plane," *IEEE Antennas and Wireless Propagation Letters*, vol. 17, no. 3, pp. 454–457, 2018.

[11] Z. Li, E. Ahmed, A. M. Eltawil, and B. A. Cetiner, "A beam-steering reconfigurable antenna for WLAN applications," *IEEE Transactions on Antennas and Propagation*, vol. 63, no. 1, pp. 24–32, 2015.

[12] H. A. Majid, M. K. A. Rahim, M. R. Hamid, and M. F. Ismail, "Frequency and pattern reconfigurable slot antenna," *IEEE Transactions on Antennas and Propagation*, vol. 62, no. 10, pp. 5339–5343, 2014.

[13] K. Trzebiatowski, M. Rzymowski, L. Kulas, and K. Nyka, "Simple 60 GHz switched beam antenna for 5G millimeter-wave applications," *IEEE Antennas and Wireless Propagation Letters*, vol. 20, no. 1, pp. 38–42, 2021.

[14] X. Jin, S. Liu, Y. Yang, and Y. Zhou, "A frequency-reconfigurable planar slot antenna using s-pin diode," *IEEE Antennas and Wireless Propagation Letters*, vol. 21, no. 5, pp. 1007–1011, 2022.

[15] P. K. Li, Z. H. Shao, Q. Wang, and Y. J. Cheng, "Frequency- and pattern-reconfigurable antenna for multistandard wireless applications," *IEEE Antennas and Wireless Propagation Letters*, vol. 14, pp. 333–336, 2015.

[16] Y. Yang and X. Zhu, "A wideband reconfigurable antenna with 360° beam steering for 802.11ac WLAN applications," *IEEE Transactions on Antennas and Propagation*, vol. 66, no. 2, pp. 600–608, 2018.

[17] M. S. Alam and A. M. Abbosh, "Wideband pattern-reconfigurable antenna using pair of radial radiators on truncated ground with switchable director and reflector," *IEEE Antennas and Wireless Propagation Letters*, vol. 16, pp. 24–28, 2017.

[18] S. I. M. Sheikh, A. A. P. Gibson, M. Basorrah, G. Alhulwah, K. Alanizi, M. Alfarsi, and J. Zafar, "Analog/digital ferrite phase shifter for phased array antennas," *IEEE Antennas and Wireless Propagation Letters*, vol. 9, pp. 319–321, 2010.

[19] H. Attia, M. Bait-Suwailam, and O. Ramahi, "Enhanced gain planar Inverted-F antenna with metamaterial superstrate for UMTS applications," in *PIERS 2010 Cambridge - Progress in Electromagnetics Research Symposium, Proceedings*, Jul 2010, pp. 494–497.

[20] L.-R. Tan, R.-X. Wu, and Y. Poo, "Magnetically reconfigurable SIW antenna with tunable frequencies and polarizations," *IEEE Transactions on Antennas and Propagation*, vol. 63, no. 6, pp. 2772–2776, 2015.

[21] F. Sultan and S. S. I. Mitu, "Superstrate-based beam scanning of a fabry–perot cavity antenna," *IEEE Antennas and Wireless Propagation Letters*, vol. 15, pp. 1187–1190, 2016.

[22] M. Su, X. Geng, Y. Zhang, and A. Wang, "Frequency-reconfigurable liquid metal magnetoelectric dipole antenna," *IEEE Antennas and Wireless Propagation Letters*, vol. 20, no. 12, pp. 2481–2485, 2021.

[23] S. Foo, "Liquid-crystal-tunable metasurface antennas," in *2017 11th European Conference on Antennas and Propagation (EUCAP)*, 2017, pp. 3026–3030.

[24] D. Pozar, "Radiation and scattering characteristics of microstrip antennas on normally biased ferrite substrates," *IEEE Transactions on Antennas and Propagation*, vol. 40, no. 9, pp. 1084–1092, 1992.

[25] P. Chen, Z. Sun, J. Jiang, H. Li, and G. Li, "A tunable broadband microstrip antenna based on ferrite material," in *2020 IEEE 4th Information Technology, Networking, Electronic and Automation Control Conference (ITNEC)*, vol. 1, 2020, pp. 1726–1729.

[26] R. Mishra, S. Pattnaik, and N. Das, "Tuning of microstrip antenna on ferrite substrate," *IEEE Transactions on Antennas and Propagation*, vol. 41, no. 2, pp. 230–233, 1993.

[27] F. A. Ghaffar, J. R. Bray, and A. Shamim, "Theory and design of a tunable antenna on a partially magnetized ferrite LTCC substrate," *IEEE Transactions on Antennas and Propagation*, vol. 62, no. 3, pp. 1238–1245, 2014.

[28] S. Yang, Y. Chen, C. Yu, Y. Gong, and F. Tong, "Design of a low-profile, frequency- reconfigurable, and high gain antenna using a varactor-loaded amc ground," *IEEE Access*, vol. 8, pp. 158 635–158 646, 2020.

[29] M. A. Abdalla and Z. Hu, "Comapct and tunable metamaterial antenna for multi-band wireless communication applications," in *2011 IEEE International Symposium on Antennas and Propagation (APSURSI)*, 2011, pp. 1054–1057.

[30] L. r. Tan, R.-x. Wu, and Y. Poo, "Magnetically reconfigurable HMSIW antenna with broadband frequency tunability," *IEEE Antennas and Wireless Propagation Letters*, vol. 15, pp. 1373–1376, 2016.

[31] S. I. Latif and S. K. Sharma, *Metamaterials in Reconfigurable Antennas*. John Wiley Sons, Ltd, 2021, ch. 9, pp. 321–340.

[32] D. Guha and Y. M. M. Antar, *Microstrip and Printed Antennas: New trends, techniques and applications*. John Wiley & Sons, Ltd, 2011, ch. 11, p. 45–386.

[33] Exxelia, *Microwave Ferrites & FDA Data sheet, YIG properties*, 2015.

[34] D. M. Pozar, *Microwave Engineering*. 4th Edition, Wiley, 2011.

[35] A. J. Baden Fuller, *Ferrites at Microwave Frequencies*. IEE Electromagnetic Waves series 23, 1987.

[36] Stanford Magnets. Neodymium magnet (NdFeB magnet). [Online]. Available: https://www.stanfordmagnets.com/common-applications-of-neodymium-magnets.html